Applied Catalysis A: General 469 (2014) 132–138

Contents lists available at ScienceDirect

Applied Catalysis A: General

journal homepage: www.elsevier.com/locate/apcata

Pd-nanoparticles supported onto functionalized poly(lactic acid)-based stereocomplexes for partial alkyne hydrogenation

Giorgio Petrucci[a], Werner Oberhauser[b,*], Mattia Bartoli[a], Guido Giachi[a], Marco Frediani[a,*], Elisa Passaglia[c], Laura Capozzoli[d], Luca Rosi[a]

[a] Dipartimento di Chimica, Università di Firenze, via della Lastruccia 13, 50019 Sesto Fiorentino, Firenze, Italy
[b] Istituto di Chimica dei Composti OrganoMetallici (ICCOM)-CNR, Via Madonna del Piano 10, 50019 Sesto Fiorentino, Firenze, Italy
[c] ICCOM-CNR, UOS Pisa, Area della Ricerca, via Moruzzi 1, 56124 Pisa, Italy
[d] Centro di Microscopie Elettroniche "Laura Bonzi" (Ce.M.E.)-ICCOM, Area di Ricerca CNR di Firenze, via Madonna del Piano 10, 50019 Sesto Fiorentino, Firenze Italy

ARTICLE INFO

Article history:
Received 15 July 2013
Received in revised form 6 September 2013
Accepted 26 September 2013
Available online 6 October 2013

Keywords:
Polyesters
Stereocomplexes
Alkyne hydrogenation
Palladium nanoparticles

ABSTRACT

Bipyridine-functionalized poly(lactic acid) (PLA)-based stereocomplexes were employed to stabilize Pd-nanoparticles (NPs). The well defined heterogeneous catalysts were suitable to catalyze the partial hydrogenation reaction (i.e. $p(H_2) = 3$ bar, 25 and 60 °C) of phenylacetylene and diphenylacetylene in THF to give styrene and *cis*-stilbene with a chemoselectivity of 96% and 91%, respectively. Since the polymer support revealed stable under real catalytic conditions, stabilizing also efficiently the Pd-NPs in the course of the catalytic reaction, the heterogeneous catalytic system was easily recyclable. The catalytic activity as well as the chemoselectivity of the supported catalyst proved to be comparable in four consecutive catalytic cycles even by recovering the catalyst in air atmosphere after each cycle.

1. Introduction

The catalytic partial hydrogenation of alkynes to alkenes is of special relevance in bulk, and fine chemical industries [1,2]. This latter catalytic process is most conveniently performed with the Lindlar catalyst (i.e. palladium nanoparticles (NPs) supported onto quinoline-promoted $CaCO_3$ which is partially poisoned with lead [3]). A further development of the latter catalyst using $BaSO_4$ as support and quinoline as modifier gave results which were found superior to that obtained by Lindlar's catalyst in terms of reproducibility and ease of preparation [4]. The presence of an organic surface modifier [5–8], which is mainly involved in the rearrangement process of the Pd-(NPs) [9] revealed mandatory for obtaining high chemo- and regioselectivity in the partial hydrogenation of terminal and internal alkynes to terminal olefins and internal *cis*-olefins, respectively, avoiding hence the over-hydrogenation of the substrate giving alkanes. The organic modifier has always to be added to the catalytic reaction solution after each catalytic cycle and consequently separated from the catalytic solution, which is a clear drawback of the latter heterogeneous catalyst. Hence other heterogeneous catalysts have been developed such as carbon-based nanomaterials [10–13], inorganic materials [14–17], functional organic polymers [18,19] (e.g. poly(ethylenimine) [20,21], polyaniline [22], poly(ethylene glycol) [23], poly(methacryalate) [24], poly(*N*-vinyl-2-pyrrolidone) [25]), resins [26–28], porous organic polymers [29,30] and organic-inorganic composite materials [31,32].

Since functional polymer-based catalytic systems generally exhibit important advantages over traditional catalysts such as: (i) the possible control of the particle shape exerted by functional groups located in the polymer chain; (ii) the improvement of catalytic selectivity; (iii) the stabilization of NPs by suppression of their aggregation [18,19,33]. In this context we propose bipyridine-functionalized poly(lactic acid) (PLA)-based stereocomplexes [34–39] as heterogeneous polymer support for Pd-(NPs), which efficiently catalyzed the partial hydrogenation of phenylacetylene and diphenylacetylene to styrene and *cis*-stilbene as major organic compounds. The effect of the Pd-(NPs)-localization in different polymer environments on the catalysts' performance was studied.

Stereocomplexation of PLA (i.e. interaction between PLA chains with opposite stereoconfiguration) which is based on the $CH_3 \ldots O$(carbonyl oxygen atom) hydrogen bonds as proved by IR-spectroscopy [40] confers high mechanical performance [41], thermal stability [42] and hydrolysis resistance [43] to PLA.

* Corresponding authors. Tel.: +39 55 5225284/+39 55 4573459; fax: +39 55 5225203/+39 55 4573531.
E-mail addresses: werner.oberhauser@iccom.cnr.it (W. Oberhauser), marco.frediani@unifi.it (M. Frediani).

0926-860X/$ – see front matter © 2013 Elsevier B.V. All rights reserved.
http://dx.doi.org/10.1016/j.apcata.2013.09.053

2. Experimental

2.1. Materials

$Pd(OAc)_2$ (OAc—acetate), L- or D-lactide, $Sn(Oct)_2$ (Oct—2-hexylhexanoate) 4,4′-dihydroxymethyl-2,2′-bipyridine were purchased from Aldrich. L- And D-lactide were sublimed before utilization and stored thereafter at 4 °C under a nitrogen atmosphere. Solvents such as *n*-hexane, $CHCl_3$, and HPLC-grade THF were purchased from Aldrich, while CH_2Cl_2 was purchased from J.T. Baker. All solvents were used without further purification.

2.2. Catalyst preparation

2.2.1. Synthesis of L-$\mathbf{L^1}$ and D-$\mathbf{L^1}$

A Schlenk tube was successively charged with L- or D-lactide (5.0 g, 34.715 mmol), 4,4′-dihydroxymethyl-2,2′-bipyridine (134.0 mg, 0.620 mmol) and $Sn(Oct)_2$ (55.9 mg, 0.181 mmol), followed by heating the resulting solid reaction mixture at 135 °C for 3 h under nitrogen. Afterwards, the reaction mixture was allowed to cool to room temperature and the sublimed lactide was removed mechanically. The crude reaction product was then dissolved in $CHCl_3$ (20.0 mL) and upon addition of *n*-hexane (50.0 mL) to the latter solution the product precipitated as white powder which was separated from solution by filtration and dried at 30 °C for 24 h. Yield (L-$\mathbf{L^1}$) = 4.728 g, (92%); yield (D-$\mathbf{L^1}$) = 4.695 g, (91%). M_n (L-$\mathbf{L^1}$) = 9500 g mol^{-1} (^{1}H NMR), 9700 g mol^{-1} (GPC-RI), polydispersity index (PDI) = 1.00; M_n (D-$\mathbf{L^1}$) = 9500 g mol^{-1} (^{1}H NMR), 10,000 g mol^{-1} (GPC-RI), PDI = 1.04. NMR data are reported in Appendices A and B.

2.2.2. Synthesis of L-$\mathbf{L^2}$ and D-$\mathbf{L^2}$

A Schlenk tube was successively charged with a (1:1) mixture of L- and D-lactide (1.1 g, 7.359 mmol), 4,4′-dihydroxymethyl-2,2′-bipyridine (247.0 g, 1.143 mmol) and $Sn(Oct)_2$ (72.2 mg, 0.234 mmol) in a dry box under nitrogen. Afterwards, the solid reaction mixture was heated at 135 °C for 3 h under nitrogen, followed by cooling to room temperature. The crude reaction product was dissolved in $CHCl_3$ (5.0 mL) and on addition of *n*-hexane (25.0 mL) an oily product precipitated which was washed with *n*-hexane (2 × 10.0 mL) and dried under vacuum. Yield: 0.950 g (73%). The degree of polymerization, determined by ^{1}H NMR spectroscopy, was found to be 12. The above isolated product was dissolved in toluene (10.0 mL) and the obtained solution was divided into two portions. To each portion was added either L-lactide or D-lactide (5.0 g, 35.0 mmol), and $Sn(Oct)_2$ (60.2 mg, 0.195 mmol). The resulting reaction mixtures were refluxed under a nitrogen atmosphere for 24 h. Afterwards, the latter reaction mixtures were allowed to cool to room temperature and the products were precipitated and washed with *n*-hexane (10.0 mL). The obtained crude products were again dissolved in CH_2Cl_2 (10.0 mL) and reprecipitated with *n*-hexane (40.0 mL) giving off-white powders which were separated by filtration and dried under vacuum at room temperature for 24 h. Yield (L-$\mathbf{L^2}$) = 4.895 g, (89%); yield (D-$\mathbf{L^2}$) = 4.917 g, (90%). M_n (L-$\mathbf{L^2}$) = 11,200 g mol^{-1} (^{1}H NMR), 10,320 g mol^{-1} (GPC-RI), PDI = 1.15; M_n (D-$\mathbf{L^2}$) = 12,300 g mol^{-1} (^{1}H NMR), 10,250 g mol^{-1} (GPC-RI), PDI = 1.33. NMR data are reported in Appendices A and B.

2.2.3. Synthesis of $\mathbf{L^a}$ and $\mathbf{L^b}$

Both (PLA)-based stereocomplexes were synthesized as follows: L-$\mathbf{L^1}$ or L-$\mathbf{L^2}$ (500 mg) were separately dissolved in CH_2Cl_2 (8.0 mL). To these latter solutions were added D-$\mathbf{L^1}$ and D-$\mathbf{L^2}$ (500 mg), respectively, dissolved in CH_2Cl_2 (8.0 mL) at room temperature. The obtained clear solutions were successively stirred for 5 min and the solvent completely evaporated by means of a vacuum pump. The obtained white-off solids were dried under vacuum at room temperature for 1 h; Yield = 980 mg (98%) ($\mathbf{L^a}$) and 960 mg (96%) ($\mathbf{L^b}$).

2.2.4. Synthesis of $Pd(OAc)_2$(L-$\mathbf{L^1}$)

In a Schlenk tube was dissolved L-$\mathbf{L^1}$ (400.0 mg, 0.042 mmol) in deareated CH_2Cl_2 (10.0 mL). To this latter solution was added $Pd(OAc)_2$ (9.90 mg, 0.044 mmol) under nitrogen and the resulting solution was allowed to stir for 3 h, followed by its concentration to dryness. The crude product was washed with diethyl ether (2 × 10.0 mL) and dried at room temperature giving a yellow powder; Yield = 395.0 mg (97%); Pd-content: 0.85 wt%. NMR data are reported in Appendices A and B.

2.2.5. Synthesis of $Pd(OAc)_2\mathbf{L^{a/b}}$ in THF

In a round-bottom flask were suspended $\mathbf{L^a}$ and $\mathbf{L^b}$ (300 mg) in THF (8.0 mL). To the latter suspensions was added $Pd(OAc)_2$ (6.96 mg, 0.031 mmol) and the resulting yellow suspensions were stirred under nitrogen for 5 h. Afterwards, the reaction mixtures were centrifuged and the supernatant decanted. The obtained solids were washed with THF (2 × 10.0 mL) and centrifuged in order to remove quantitatively uncoordinated $Pd(OAc)_2$. Yield = 295.0 mg (96%) ($Pd(OAc)_2\mathbf{L^a}$) and 290.0 mg (94%) ($Pd(OAc)_2\mathbf{L^b}$).

2.2.6. Synthesis of $Pd(OAc)_2\mathbf{L^{(a/b)'}}$ in CH_2Cl_2

$\mathbf{L^a}$ and $\mathbf{L^b}$ (15.0 mg) were suspended separately in a Schlenk tube in deareated CH_2Cl_2 (3.0 mL). To the latter suspensions was added $Pd(OAc)_2$ (1.0 mg) and the resulting yellow suspensions were stirred under nitrogen for 3 h. Afterwards, the suspensions were concentrated to dryness and the obtained yellow solids were suspended in CD_2Cl_2 in order to carry out ^{1}H NMR spectroscopic measurements.

2.2.7. Synthesis of Pd@$\mathbf{L^{a/b}}$ and Pd@$\mathbf{L^{(a/b)'}}$

In an autoclave $Pd(OAc)_2\mathbf{L^{a/b}}$ (400.0 mg) was suspended in deareated THF (20.0 mL) at room temperature. The autoclave was then pressurized with dihydrogen (15.0 bar) and stirred at room temperature for 12 and 16 h. Afterwards, the dihydrogen pressure was released and the obtained black suspension was transferred into a Schlenk tube, where the solvent was completely removed. The obtained gray powder was washed with diethyl ether (2 × 10.0 mL) and then dried under vacuum giving Pd@$\mathbf{L^{a/b}}$. An identical synthesis procedure using CH_2Cl_2 instead of THF gave Pd@$\mathbf{L^{a/b'}}$. (ICP-OES)-analyses of Pd@$\mathbf{L^{a/b}}$ and Pd@$\mathbf{L^{(a/b)'}}$ showed a Pd-content of 0.48 wt%.

2.3. Catalyst characterization

^{1}H and $^{13}C\{^1H\}$ NMR data were obtained with a Bruker Avance DRX-300 spectrometer at 300.13 and 75.47 MHz, respectively. CD_2Cl_2 used for NMR experiments was dried over molecular sieves and chemical shifts are reported in ppm (δ).

(GPC)-analyses were per formed with a GPC system, equipped with a Waters Binary HPLC 1525 pump, a manual injector with a six-way valve and a 200 μL loop, three in-series connected Shodex KF-802.5, KF-803 and KF-804 columns (length: 300 mm each, inner diameter: 8.0 mm, 24,500 theoretical plates, exclusion limit for PS up to 400 000 g mol^{-1}; a RI detector (Optilab T-rEX^{TM}, Wyatt Technology). HPLC-grade THF with a water content of maximal 0.1 vol% was used as eluent at a constant flux of 1.0 mL min^{-1}, keeping the columns at 30.0 °C by a thermostat. The GPC system was calibrated using polystyrene (PS) as standard.

(XRPD)-spectra were acquired on a X'Pert PRO (PANalytical) powder diffractometer in a 2Θ range from 5.0° to 60.0° with a step size of 0.1050° and a counting time of 428.9 s, using Cu *K*α radiation (λ = 1.541874 Å).

Table 1
(DSC)-data for L-**L**^{1}, L-**L**^{2}, **L**^{a}, **L**^{b}, Pd@**L**^{a} and Pd@**L**^{b}.

Sample	T_g (°C)	T_c (°C)/ΔH(J g^{-1})	T_m (°C)/ΔH(J g^{-1})
L-**L**^{1}	49.7	111.5/−40.4[§]	145.4; 157.6/40.1
L-**L**^{2}	51.0	118.4/−39.6[§]	148.6; 156.8/39.6
L^{a}	n.d.	101.4/−42.6	223.5/60.7[*]
L^{b}	n.d.	95.5/−34.3	217.7/69.7[*]
Pd@**L**^{a}	n.d.	181.0/−88.6	224.4/93.4
Pd@**L**^{b}	n.d.	142.2/−68.6	216.5/68.7

[§] Cold crystallization.
[*] 1st heating.

Table 2
(TG)-data for L-**L**^{1}, L-**L**^{2}, **L**^{a}, **L**^{b}, Pd@**L**^{a} and Pd@**L**^{b}.

Sample	T (°C) (5% weight loss)	T (°C) (peak)	Residue (wt%)
L-L^{1}	215.1	261.8	3.2
L-L^{2}	217.3	265.8	2.6
L^{a}	214.9	273.1	2.3
L^{b}	203.5	267.5	2.2
Pd@L^{a}	293.8	357.9	4.7
Pd@L^{b}	253.7	295.1	3.3

(ICP-OES)-analyses were carried out on an ICP apparatus of the type Perkin Elmer Optima 2000 OES DV.

(TEM)-measurements were carried out on a TEM PHILIPS CM 12, equipped with an OLYMPUS Megaview G2 camera and using an accelerating voltage of 100 kV. Samples for (TEM)-analyses were prepared by depositing a drop of an ethanol suspension of the sample on a holey and lacey film on the carbon support of 200 mesh Cu grids, followed by the evaporation of the solvent.

(DSC)-analyses were carried out under an atmosphere of nitrogen with a Perkin Elmer instrument calibrated with In and Pd. For the (DSC)-analyses of L-**L**^{1} and L-**L**^{2} the following heating program was applied: 1st heating: 30.0 to 200.0 °C at 20.0 °C min^{-1} holding the latter temperature for 1.0 min, followed by cooling the sample to 30.0 °C and holding the latter temperature for 5.0 min; 2nd heating: from 30.0 to 200.0 °C at a heating rate of 20.0 °C min^{-1}.

For the (DSC)-analyses of **L**^{a}, **L**^{b}, Pd@**L**^{a}, and Pd@**L**^{b} the following heating program was applied: 1st heating: 30.0 to 235.0 °C at 20.0 °C min^{-1} holding the latter temperature for 1.0 min, followed by cooling the sample to 30.0 °C and holding the latter temperature for 5.0 min; 2nd heating: from 30.0 to 235.0 °C at a heating rate of 20.0 °C min^{-1}. Relevant (DSC)-data are summarized in Table 1.

(TG)-analyses were performed with a Seiko TG/DTA 7200 instrument in the temperature interval from 30 to 700 °C with a heating rate of 10 °C min^{-1} under a nitrogen atmosphere. Relevant (TG)-data are compiled in Table 2.

2.4. Catalytic partial hydrogenation of phenylacetylene and diphenylacetylene in THF

Pd@**L**$^{a/b}$ and Pd@**L**$^{(a/b)'}$ (0.834 μmol of Pd) were introduced into a teflonated stainless steel autoclave (80.0 mL) which was then sealed and evacuated. Afterwards, deareated THF (10.0 mL) solutions of the substrates (4.0 mmol) were introduced into the autoclave by suction. The autoclave was then charged with dihydrogen (3 bar) and heated at the desired temperature with stirring. After the desired reaction time the autoclave was cooled to 5 °C by means of a water-ice bath, dihydrogen vented and the catalytic solution analyzed by GC and GC-MS.

(GC)-analyses were performed with a Shimadzu 2010 gas chromatograph equipped with a flame ionization detector and a 30 m (0.25 mm i.d., 0.25 μm film thickness) VF-WAXms capillary column, while (GC-MS)-analyses were carried out with a Shimadzu QP 5000 apparatus, equipped with a 30 m (0.32 mm i.d., 0.50 μm film thickness) CP-WAX 52 CB WCOT-fused silica column.

2.5. Catalyst recycling experiments with Pd@**L**$^{b'}$ in air atmosphere

Pd@**L**$^{b'}$ (18.5 mg, 0.834 μmol) was introduced into a teflonated steel autoclave (80.0 mL) along with the THF (10 mL) solution of phenylacetyelene or diphenylacetylene (4.0 mmol) in air atmosphere. The autoclave was then successively sealed, heated to 25 or 60 °C and pressurized with dihydrogen (3.0 bar). After a reaction time of 1 h, the autoclave was successively cooled to 5 °C by means of a water–ice bath, dihydrogen vented off and the content of the autoclave centrifuged in order to separate the solid supported catalyst from the liquid. The clear catalyst solution was analyzed by GC. The recovered solid was then suspended in THF (10.0 mL), the resulting suspension centrifuged and the supernatant removed in order to quantitatively remove the organic substrate and/or product. Afterwards, the recovered solid was placed again in the autoclave followed by the addition of a THF (10 mL) solution of the appropriate substrate (4.0 mmol) in air atmosphere. The further proceeding for the next catalytic run corresponds to that reported above.

3. Results and discussion

As shown in Scheme 1a, two different types of PLA-based macroligands (i.e. L/D-**L**^{1} and L/D-**L**^{2}) were synthesized by a Sn(Oct)$_2$-catalyzed ring opening polymerization (ROP) of L/D-lactide [44], using 4,4′-dihydroxymethyl-2,2′-bipyridine as initiator. The macroligands L/D-**L**^{1} are build up by isotactic PLA which is characterized by a molar mass (M_n) of 9500 g mol^{-1}, while L/D-**L**^{2} exhibited atactic PLA (i.e. ca. 12 lactide units as determined by ^{1}H NMR spectroscopy), directly linked to the bipyridine functional moiety. This latter PLA spacer is directly linked to a block of isotactic PLA with a polymer length comparable to that found in L/D-**L**^{1}. The successful covalent anchoring of the bipyridine functionality to the PLA polymer chain was proved by acquiring ^{1}H-NMR spectra of L/D-**L**^{1} and L/D-**L**^{2} which showed for the benzyl hydrogen atoms a singlet centered at 5.30 ppm, whereas the same hydrogen atoms showed for 4,4′-dihydroxymethyl-2,2′-bipyridine a ^{1}H NMR doublet at 4.85 ppm (J = 4.8 Hz)) [45,46].

By mixing CH_2Cl_2 solutions of macroligands of opposite stereoisomerism (Scheme 1b) in an 1:1 molar ratio and by completely evaporating the solvent of the stereocomplex solution, **L**^{a} and **L**^{b} were obtained as off-white solids with 98% yield.

X-ray powder diffraction (XRPD)-spectra of **L**^{a} and **L**^{b} exclusively showed the Bragg reflections for (PLA)-based stereocomplexes centered at 2Θ: 11.8° (1 1 0), 20.5° (3 0 0)+(0 3 0)+(1 2 1) and 23.6° (2 2 0). Importantly the broad hump at 32.5° (2Θ), which corresponds to the (2 3 1) and (1 0 3) reflections, is detectable only when the solvent slowly evaporates from stereocomplex solution (Fig. 1, traces a and b) [34–37,39].

In accordance with the (XRPD) results, (DSC)-analyses carried out on isolated **L**$^{a/b}$ (Table 1) showed the absence of an exothermic peak at ca 160 °C which is characteristic for the melting point of isotactic PLA [36]. This experimental finding proves that both stereoisomers of PLA are involved in the stereocomplex formation. As a result, melting points of 223° and 218° for **L**^{a} and **L**^{b}, respectively, were found, as far as the first heating is concerned [38].

The reaction of a suspension of **L**^{a} and **L**^{b} in THF with Pd(OAc)$_2$ gave the corresponding Pd-complexes (i.e. Pd(OAc)$_2$**L**$^{a/b}$) as pale yellow solids (Scheme 1c) which were washed several times with fresh THF in order to remove uncoordinated Pd(OAc)$_2$. **L**^{a} and **L**^{b} proved to be insoluble in THF and CH_2Cl_2 even at 60 °C. Importantly, the latter stereocomplexes showed good swelling properties in CH_2Cl_2, which was exploited to study the coordination of Pd(OAc)$_2$

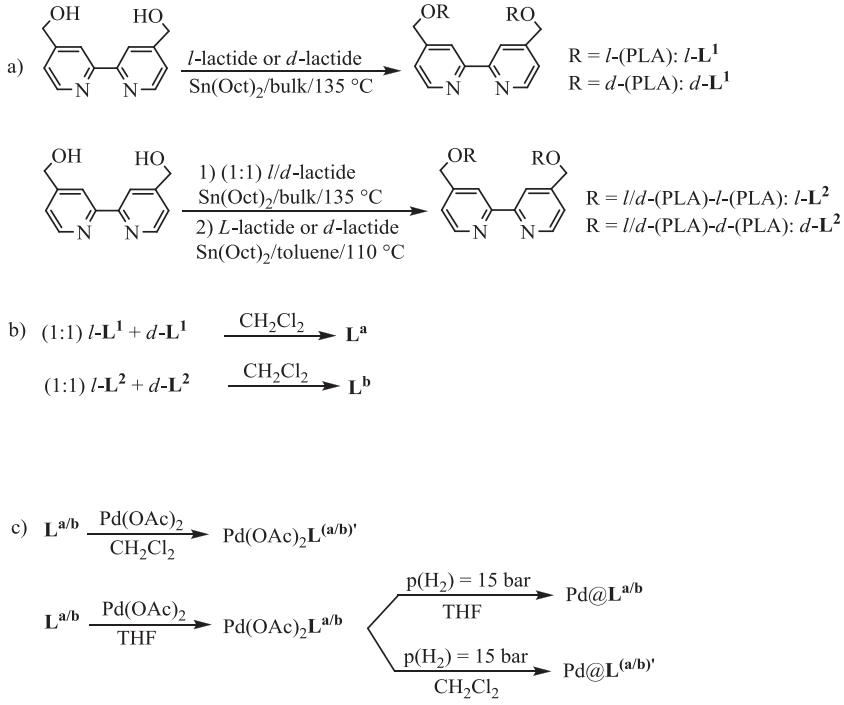

Scheme 1. Syntheses of PLA-based macroligands, stereocomplexes, and stereocomplex-stabilized Pd-(NPs).

to $\mathbf{L^a}$ and $\mathbf{L^b}$ by ^{1}H NMR spectroscopy. To this purpose, $\mathbf{L^{a/b}}$, suspended in CH_2Cl_2, reacted with $Pd(OAc)_2$ giving $Pd(OAc)_2\mathbf{L^{(a/b)'}}$ which was directly subjected to ^{1}H NMR measurements carried out in CD_2Cl_2. For comparison reason, $Pd(OAc)_2$(L-$\mathbf{L^1}$), which is completely soluble in CD_2Cl_2, was synthesized. The corresponding ^{1}H NMR spectra are compiled in Fig. 2.

As shown in Fig. 2, the ^{1}H NMR signals assigned to the bipyridine moiety shifted upon coordination to $Pd(OAc)_2$ (Fig. 2, trace b vs. a; d vs. c and f vs. e), confirming the successful coordination of $Pd(OAc)_2$ to the bipyridine units of $\mathbf{L^a}$ and $\mathbf{L^b}$. Moreover, the broad ^{1}H NMR signals for coordinated bipyridine in $Pd(OAc)_2\mathbf{L^{(a/b)'}}$ confirmed the anisotropic chemical environment in swollen $\mathbf{L^a}$ and $\mathbf{L^b}$. A $^{13}C\{^1H\}$ NMR spectrum of isolated $Pd(OAc)_2$(L-$\mathbf{L^1}$) acquired in CD_2Cl_2 proved the symmetrical coordination of $Pd(OAc)_2$ to the bipyridine moiety, showing for both coordinated acetate moieties a singlet at 23.0 (i.e CH_3COO) and 177.7 ppm (i.e. CH_3COO).

THF and CH_2Cl_2 suspensions of $Pd(OAc)_2\mathbf{L^{(a/b)}}$ were treated with dihydrogen (15 bar) in an autoclave at room temperature for 12 h, yielding Pd@$\mathbf{L^{a/b}}$ and Pd@$\mathbf{L^{(a/b)'}}$ (i.e. Pd-(NPs) stabilized by $\mathbf{L^{a/b}}$), respectively (Scheme 1c). Accordingly, ^{1}H NMR spectra of Pd@$\mathbf{L^{a/b}}$ and Pd@$\mathbf{L^{(a/b)'}}$ acquired in CD_2Cl_2 after a reduction reaction lasting 12 h showed for the bipyridine hydrogen atoms chemical shifts which are typically found for uncoordinated $\mathbf{L^a}$ and $\mathbf{L^b}$ (Appendices A and B), confirming hence the successful reduction of coordinated $Pd(OAc)_2$ to $\mathbf{L^a}$/$\mathbf{L^b}$-supported NPs.

(XRPD)-measurements carried out on isolated Pd@$\mathbf{L^{a/b}}$ confirmed the stability of the stereocomplex under reductive experimental conditions (Fig. 1, traces c/d vs. a/b), while (TEM)-images of Pd@$\mathbf{L^{a/b}}$ and Pd@$\mathbf{L^{(a/b)'}}$ proved the presence of Pd-(NPs) in the latter samples (Fig. 3).

From a comparison of the (TEM)-histograms (Fig. 3) emerged that the reduction of $Pd(OAc)_2\mathbf{L^{a/b}}$, carried out in CH_2Cl_2, led to the same average Pd-(NP) size in Pd@$\mathbf{L^{a'}}$ and Pd@$\mathbf{L^{b'}}$ (Fig. 3c/d). This experimental fact is rationalized by the good swelling properties of $\mathbf{L^a}$/$\mathbf{L^b}$ in CH_2Cl_2 forming gels [34,47], while $\mathbf{L^a}$/$\mathbf{L^b}$ do not

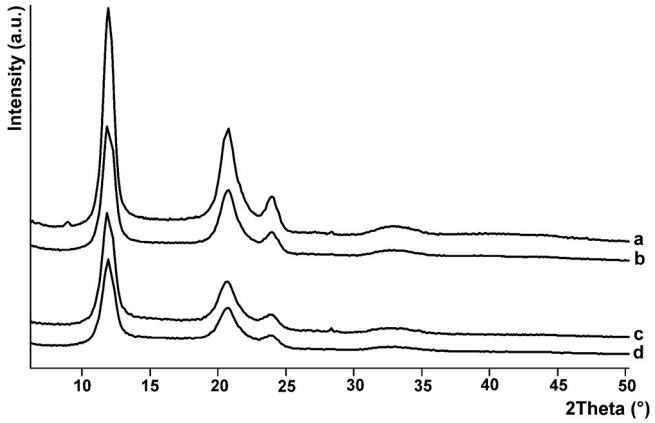

Fig. 1. (XRPD)-traces of $\mathbf{L^a}$ (a), $\mathbf{L^b}$ (b), Pd@$\mathbf{L^a}$ (c) and Pd@$\mathbf{L^b}$ (d).

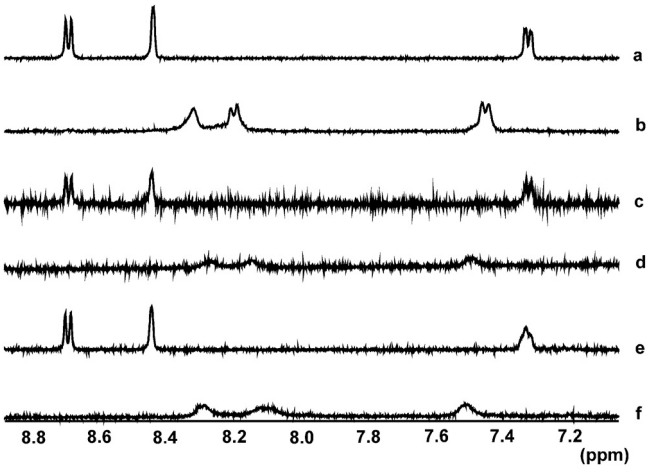

Fig. 2. ^{1}H NMR spectra acquired in CD_2Cl_2 in the chemical shift range from 7.06 to 8.89 ppm. L-$\mathbf{L^1}$ (a), $Pd(OAc)_2$(L-$\mathbf{L^1}$) (b), $\mathbf{L^a}$ (c), $Pd(OAc)_2\mathbf{L^{a'}}$ (d), $\mathbf{L^b}$ (e) and $Pd(OAc)_2\mathbf{L^{b'}}$ (f).

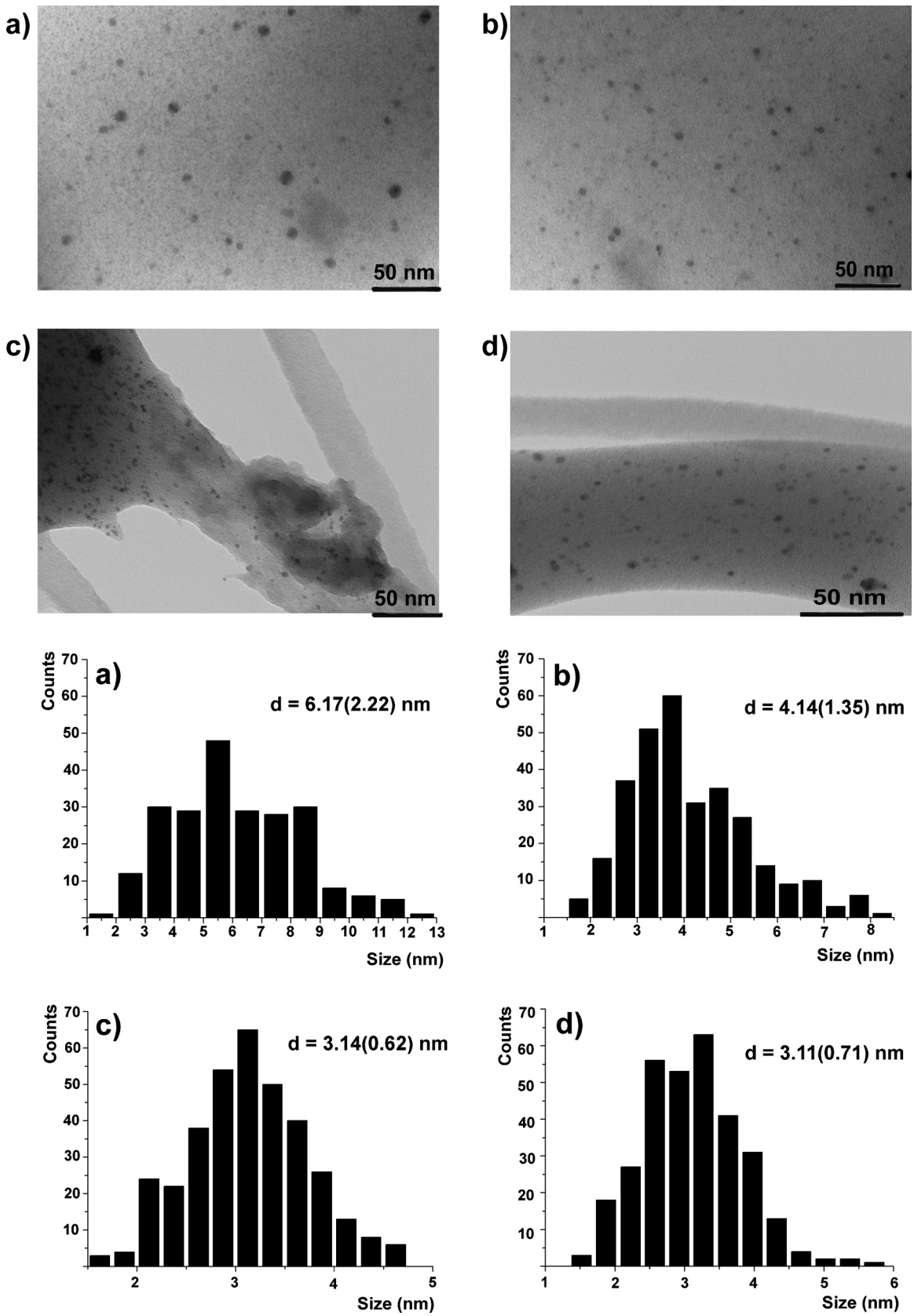

Fig. 3. (TEM)-images and histograms of Pd@$\mathbf{L}^{a}$ (a), Pd@$\mathbf{L}^{b}$ (b), Pd@$\mathbf{L}^{a'}$ (c) and Pd@$\mathbf{L}^{b'}$ (d).

swell in THF. As a consequence, the reduction of $Pd(OAc)_2$**L**^{a} (i.e. **L**^{a} contains no amorphous PLA-spacer) in THF led to Pd@**L**^{a} which is characterized by the biggest Pd-(NP) average size combined with the largest Pd-(NP) distribution among the cases studied. In fact, a rigid polymer structure without swelling properties in a given solvent slows down the kinetic of the Pd(II) reduction, leading thus to the formation of large Pd-(NPs) particles size [33].

Importantly, the presence of Pd-(NPs) anchored onto **L**$^{a/b}$ increased significantly the thermal stability of the latter stereocomplexes as proved by (TG)-analyses carried out on Pd@**L**$^{a/b}$ and on **L**$^{a/b}$ (Table 2). As a result, the onset degradation temperature of Pd@**L**$^{a/b}$ was 50–80 °C higher compared to that of **L**$^{a/b}$ and the fastest decomposition rate observed at *T* (peak) followed the same trend (i.e. 357.9 (Pd@**L**^{a}) vs. 273.1 °C (**L**^{a}) and 295.1 (Pd@**L**^{b}) vs. 267.5 °C (**L**^{b}) (Table 2). Comparable experimental results were found for poly(ethylene glycol)-stabilized Pd-(NPs), provided the palladium was finely dispersed throughout the polymer matrix [46].

Pd@**L**$^{a/b}$ and Pd@**L**$^{(a/b)'}$ were applied to catalyze the partial hydrogenation of phenylacetylene (A) and diphenylacetylene (B) in THF to give styrene and *cis*-stilbene as the major organic compounds. In order to ensure the absence of gas-liquid diffusion limitations during the catalytic reactions, stirrer velocity (500–1000 rpm) and dihydrogen pressure (3–8 bar) were screened. As a result, we found almost identical substrate conversions and chemoslectivities in the latter range of experimental conditions. The experimental results compiled in Table 3 are thus carried out with a stirrer velocity of 700 rpm and a dihydrogen pressure of 3 bar.

The TOF-values reported in Table 3 refer to the substrate-accessible amount of supported palladium, which was determined by (TEM)-measurements, applying the following equation: $D = 0.9/d$, where *D* is the palladium dispersion and *d* is the mean diameter in nm of the Pd-(NPs) [11,16].

A screening of the catalysts' performance exhibited for **L**^{b}-based catalysts (i.e. Pd@**L**^{b} and Pd@**L**$^{b'}$) a significantly higher catalytic activity compared to the **L**^{a} counterparts, regardless of the substrate and reaction temperature employed (Table 3, entries 3/4 vs. 1/2 and 9/10 vs. 7/8). The same trend applies to the chemoselectivity of styrene formation and to a lesser extent to the formation of *cis*-stilbene. Since Pd@**L**$^{a'}$ and Pd@**L**$^{b'}$, which were obtained by an identical reduction procedure in CH_2Cl_2, show an identical palladium distribution (*D*) of 0.289 it is evident that the significantly higher substrate conversion found for Pd@**L**$^{b'}$ compared to Pd@**L**$^{a'}$ is due to an easier access of the Pd-(NPs), which are embedded in the amorphous (i.e. atactic) polymer matrix of **L**^{b}, by the substrates. This latter experimental fact, corroborates the importance of the nano-environment of a functionalized polymer phase for the substrate migration and thus for the catalytic activity of supported Pd-(NPs) [19,27] (Scheme 2).

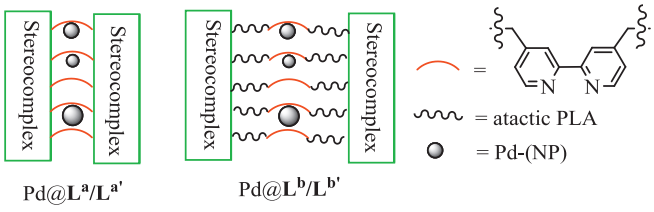

Scheme 2. **L**^{a} vs. **L**^{b}-based Pd-catalysis.

Analogous catalytic reactions carried out with Pd@**L**$^{a'}$ and Pd@**L**$^{b'}$ obtained after 12 and 16 h of dihydrogen reduction, gave comparable catalytic results in terms of catalytic activity and chemo- or regioselectivity. This experimental fact is indicating that the amount of residual Pd(II) located on the Pd-(NPs), if any, is negligible for the observed catalytic outcome and that Pd(0) is the effective catalytic species.

Since phenylacteylene is known to be structure insensitive regarding hydrogenation reactions with Pd-(NPs) in the size range from 2.5 to 5.6 nm [48], the significantly lower chemoselectivity for phenylacetylene hydrogenation of Pd@**L**$^{a/a'}$ compared to Pd@**L**$^{b/b'}$ is due to the hindered access of phenylacetylene to Pd-(NPs) in **L**^{a} (Scheme 2), fostering hence the hydrogenation of Pd-surface-adsorbed styrene to ethyl benzene instead of replacing adsorbed styrene by phenylacetylene [11]. (XRPD)-analyses carried out on recovered Pd@**L**^{a} and Pd@**L**^{b} after diphenylacetylene hydrogenation at 60 °C for 1 h confirmed the excellent stability of the organic support under real hydrogenation reaction conditions (Fig. 4).

The Pd-leaching into the THF solution of Pd@**L**^{a} and Pd@**L**^{b}-catalyzed diphenylacetylene hydrogenation reactions carried out at 60 °C for 1 and 2 h was followed by (ICP-OES)-analyses, carried out on the catalytic THF solutions. As a result, the Pd@**L**^{b}-catalyzed reactions showed slightly higher values for the Pd leaching compared to Pd@**L**^{a} (i.e. Pd@**L**^{a}: 0.8 ppm (1 h), 2.8 ppm (2 h); Pd@**L**^{b}: 1.8 ppm (1 h), and 3.8 ppm (2 h)).

Catalyst recycling experiments with Pd@**L**$^{b'}$ were carried out at 25 and 60 °C by preparing the catalyst suspension in air atmosphere. As a result, the catalytic activity as well as the chemo- and stereoselectivity of the partial hydrogenation reactions dropped

Table 3
Partial hydrogenation of selected alkynes by Pd@**L**$^{a/b}$ and Pd@**L**$^{(a/b)'}$[a].

Entry	Catalyst	Substrate	Conv. (%)/TOF[b]		$Sel_{(olefin)}$(%)/$Sel_{(cis\text{-}isomer)}$ (%)	
			1 h	2 h	1 h	2 h
1	Pd@**L**^{a}	A	11/3612	17/2790	89	87
2	Pd@**L**$^{a'}$	A	14/2340	28/2340	88	85
3	Pd@**L**^{b}	A	41/9065	67/7407	96	95
4	Pd@**L**$^{b'}$	A	44/6560	62/4623	95	95
5[c]	Pd@**L**$^{b'}$	A	42/6264	–	94	–
6[d]	Pd@**L**$^{b'}$	A	40/5965	–	94	–
7[e]	Pd@**L**^{a}	B	28/9195	39/6404	90/91	92/92
8[e]	Pd@**L**$^{a'}$	B	29/4847	n.d.	91/91	n.d.
9[e]	Pd@**L**^{b}	B	76/11,335	100/n.d.	90/94	85/95
10[e]	Pd@**L**$^{b'}$	B	86/12,826	n.d.	90/94	n.d.
11[c,e]	Pd@**L**$^{b'}$	B	83/12,380	–	90/94	–
12[d,e]	Pd@**L**$^{b'}$	B	78/11,633	–	89/93	–

[a] Pd (0.834 μmol); substrate: A (phenylacetylene); B (diphenylacetylene) (4.0 mmol); THF (10.0 mL); $p(H_2)$ (3 bar); *T* (25 °C). Catalytic suspension prepared under nitrogen.
[b] TOF defined as mmol(product) × (mmol(Pd) × h)$^{-1}$, with mmol(Pd) = mmol of substrate-accessible Pd.
[c] 1st catalytic cycle with catalytic suspension prepared in air atmosphere.
[d] 4th catalytic cycle with catalytic suspension prepared in air atmosphere.
[e] *T* (60 °C).

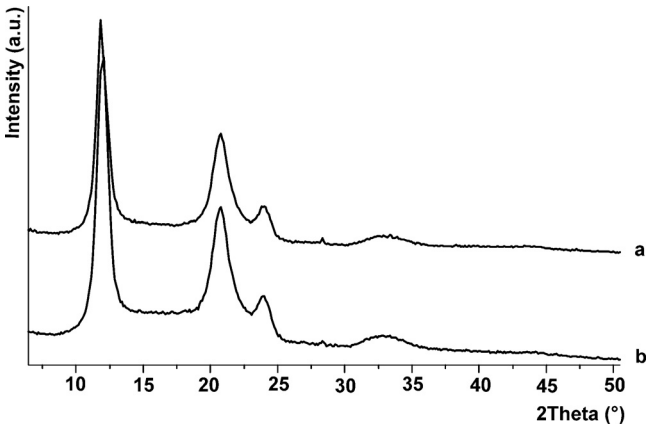

Fig. 4. (XRPD)-spectra of recovered Pd@**L**[a] (a) and Pd@**L**[b] (b) after catalysis at 60 °C.

only slightly within four consecutive catalytic runs (Table 3, entry 6 vs. 5 and 12 vs. 11).

A comparison of our catalytic results with those reported in the literature (i.e catalytic results obtained under comparable experimental conditions) revealed that: (i) Functional polymer-based catalysts gave, as expected, comparable chemoselectivies for styrene and *cis*-stilbene, but lower catalytic conversions (i.e. TOF < 1700 h^{-1}), due to serious substrate diffusion limitations [20,21,27]; (ii) Pd-(NPs) supported onto carbon without additional organic modifier led to much lower chemoselectivities (i.e styrene (<80%) [12,13] and *cis*-stilbene (85%) [12]) compared to our functional-polymer based catalytic system; (iii) silica-dendrimer core–shell microspheres [32], which is one of the best performing catalyst for at least the partial hydrogenation of phenylacetylene is outperforming our catalytic system, showing high phenylacetylene conversion (i.e. TOF = 16,000 h^{-1}) and chemoselectivity for styrene of almost 100%.

4. Conclusions

We showed that: (i) Functionalized (PLA)-based stereocomplexes are easily accessible and robust under real catalytic hydrogenation reaction conditions; (ii) The presence of an atactic PLA-based spacer in between the functional group and the stereocomplex positively steers the Pd-(NPs)-catalyzed partial hydrogenation reaction of phenylacetylene and diphenylacetylene in terms of catalytic activity, chemo-, and stereoselectivity; (iii) The polymer-based heterogeneous catalysts proved to be recyclable by a simple filtration process and to maintain their performance for at least four consecutive catalytic reactions, even if the catalyst is recovered in air atmosphere.

Acknowledgments

The authors thank M.C. Mascherpa for carrying out the (ICP-OES)-analyses.

Appendix A. Supplementary data

Supplementary data associated with this article can be found, in the online version, at http://dx.doi.org/10.1016/j.apcata.2013.09.053.

References

[1] M. Crespo-Quesada, F. Cádenas-Lizana, A.-L. Dessimoz, L. Kiwi-Minsker, ACS Catal. 12 (2012) 1773–1786.
[2] B. Chen, U. Dingerdissen, J.G.E. Krautler, H.G.J. Lansink Rotgerink, K. Möbus, D.J. Ostgard, P. Panster, T.H. Riermeier, S. Seebald, T. Tacke, H. Trauthwein, Appl. Catal., A: Gen. 280 (2005) 17–46.
[3] H. Lindlar, Helv. Chim. Acta 57 (1952) 446–450.
[4] D.J. Cram, N.L. Allinger, J. Am. Chem. Soc. 78 (1956) 2518–2524.
[5] S.G. Kwon, G. Krylova, A. Sumer, M.M. Schwartz, E.E. Bunel, Ch.L. Marshall, S. Chattopadhyay, B. Lee, J. Jellinek, E.V. Shevchenko, Nano Lett. 12 (2012) 5382–5388.
[6] T. Mallat, A. Baiker, Appl. Catal., A: Gen. 200 (2000) 3–22.
[7] R. Tschan, M.M. Schubert, A. Baiker, W. Bonrath, H. Lansink-Rotgerink, Catal. Lett. 75 (2001) 31–36.
[8] J.G. Ulan, E. Kuo, W.F. Maier, J. Org. Chem. 52 (1987) 3126–3132.
[9] W.F. Maier, S.J. Chettle, R.S. Rai, G. Thomas, J. Am. Chem. Soc. 108 (1986) 2608–2616.
[10] A. Jung, A. Jess, T. Schubert, W. Schütz, Appl. Catal., A: Gen. 362 (2009) 95–105.
[11] S. Domínguez-Domínguez, Á. Berenguer-Murcia, B.K. Pradhan, Á. Linares-Solano, D. Cazorla-Amorós, J. Phys. Chem. C 112 (2008) 3827–3834.
[12] E.V. Starodubtseva, M.G. Vinogradov, O.V. Turova, N.A. Bumagin, E.G. Rakov, V.I. Sokolov, Catal. Commun. 10 (2009) 1441–1442.
[13] S.D. Jackson, L.A. Shaw, Appl. Catal., A: Gen. 134 (1996) 91–99.
[14] B.M. Choudary, M. Lakshmi Kantam, N. Mahender Reddy, K. Koteswara Rao, Y. Haritha, V. Bhaskar, F. Figueras, A. Tuel, Appl. Catal., A: Chem. 181 (1999) 139–144.
[15] Á. Mastalir, Z. Király, F. Berger, Appl. Catal., A: Gen. 269 (2004) 161–168.
[16] S. Domínguez-Domínguez, Á. Berenguer-Murcia, Á. Linares-Solano, D. Cazorla-Amorós, J. Catal. 257 (2008) 87–95.
[17] Ch. Na-Chiangmai, N. Tiengchad, P. Kittisakmontree, O. Mekasuwandumrong, J. Powell, J. Panpranot, Catal. Lett. 141 (2011) 149–1155.
[18] M. Králik, A. Biffis, J. Mol. Catal. A: Chem. 177 (2001) 113–138.
[19] Y.T. Vu, J.E. Mark, Colloid Polym. Sci. 282 (2004) 613–619.
[20] H. Sajiki, S. Mori, T. Ohkubo, T. Ikawa, A. Kume, T. Maegawa, Y. Monguchi, Chem. Eur. J. 14 (2008) 5109–5111.
[21] S. Mori, T. Ohkubo, T. Ikawa, A. Kume, T. Maegawa, Y. Monguchi, H. Sajiki, J. Mol. Catal. A: Chem. 307 (2009) 77–87.
[22] Y. Gao, Ch.-A. Chen, H.-M. Gau, J.A. Bailey, E. Akhadov, D. Williams, H.-L. Wang, Chem. Mater. 20 (2008) 2839–2844.
[23] S. Chandrasekhar, Ch. Narsihmulu, G. Chandrashekar, T. Shyamsunder, Tetrahedron Lett. 45 (2004) 2421–2423.
[24] M.M. Dell'Anna, M. Gagliardi, P. Mastrorilli, G.P. Suranna, C.F. Nobile, J. Mol. Catal. A: Chem. 158 (2000) 515–520.
[25] C. Evangelisti, N. Panziera, A. D'Alessio, L. Bertinetti, M. Botavina, G. Vitulli, J. Catal. 272 (2010) 246–252.
[26] C. Moreno Marrodan, D. Berti, F. Liguori, P. Barbaro, Catal. Sci. Technol. 2 (2012) 2279–2290.
[27] A. Drelinkiewicz, W. Stanuch, A. Knapik, A. Ghanem, R. Kosydar, A. Bukowska, W. Bukowska, J. Mol. Catal. A: Chem. 300 (2009) 8–18.
[28] A. Drelinkiewicz, A. Knapik, W. Stanuch, J. Sobczak, A. Bukowska, W. Bukowska, React. Funct. Polym. 68 (2008) 1652–1664.
[29] P. Kaur, J.T. Hupp, S.T. Nguyen, ACS Catal. 1 (2011) 819–835.
[30] W. Liu, C. Otero Arean, S. Bordiga, E. Groppo, A. Zecchina, ChemCatChem 3 (2011) 222–226.
[31] W. Long, N.A. Brunelli, S.A. Didas, E.W. Ping, Ch.W. Jones, ACS Catal. 3 (2013) 1700–1708.
[32] A.V. Biradar, A.A. Biradar, T. Asefa, Langmuir 27 (2011) 14408–14418.
[33] J.M. Campelo, D. Luna, R. Luque, J.M. Marinas, A.A. Romero, ChemSusChem 2 (2009) 18–45.
[34] H. Tsuji, Macromol. Biosci. 5 (2005) 569–597.
[35] S. Saeidlou, M.A. Huneault, H. Li, P. Sammut, C.B. Park, Polymer 53 (2012) 5816–5824.
[36] Y. Ikada, K. Jamshidi, H. Tsuji, S.-H. Hyon, Macromolecules 20 (1987) 904–906.
[37] D. Brizzolara, H.-J. Cantow, K. Diederichs, E. Keller, A.J. Domb, Macromolecules 29 (1996) 191–197.
[38] J. Sun, J. Shao, S. Huang, B. Zhang, G. Li, X. Wang, X. Chen, Mater. Lett. 89 (2012) 169–171.
[39] D. Sawai, Y. Tsugane, M. Tamada, T. Kanamoto, M. Sungil, S.-H. Hyon, J. Polym. Sci., Part B: Polym. Phys. 45 (2007) 2632–2639.
[40] J. Zhang, H. Sato, H. Tsuji, I. Noda, Y. Ozaki, Macromolecules 38 (2005) 1822–1828.
[41] H. Tsuji, Y. Ikada, Polymer 40 (1999) 6699–6708.
[42] H. Yamane, K. Sasai, Polymer 44 (2003) 2569–2575.
[43] H. Tsuji, Polymer 43 (2002) 1789–1796.
[44] H.R. Kriecheldorf, I. Kreiser-Saunders, C. Boettcher, Polymer 36 (1995) 1253–1259.
[45] G. Giachi, M. Frediani, W. Oberhauser, E. Passaglia, J. Polm. Sci., Part A: Polym. Chem. 49 (2011) 4708–4713.
[46] G. Giachi, M. Frediani, W. Oberhauser, E. Passaglia, J. Polm. Sci., Part A: Polym. Chem. 50 (2012) 2725–2731.
[47] H. Tsuji, F. Horii, S.-H. Hyon, Y. Ikada, Macromolecules 24 (1991) 2719–2724.
[48] D. Mei, P.A. Sheth, M. Neurock, C.M. Smith, J. Catal. 242 (2006) 1–15.